

## GENERAL THEORETICAL ANALYSIS OF FOUR-CONNECTED POLYHEDRAL MOLECULES

ROY L. JOHNSTON and D. MICHAEL P. MINGOS\*

*Inorganic Chemistry Laboratory, University of Oxford, South Parks Road, Oxford OX1 3QR (Great Britain)*

(Received August 14th, 1984)

### Summary

Molecular orbital calculations on four-connected polyhedral molecules have resulted in the following generalisations. Spherical four-connected transition metal carbonyl polyhedra are characterised by  $14n + 2$  electrons and their Main Group analogues by  $4n + 2$  electrons. Non-spherical four-connected polyhedra have variable electron counts of  $14n$  to  $14n + 4$  (or  $4n$  to  $4n + 4$ ). These generalisations have been analysed in terms of Stone's Tensor Surface Harmonic Theory. The development of electron counting rules for condensed polyhedra derived from four-connected polyhedral fragments is also described.

---

During the last ten years the structural diversity shown by transition metal cluster compounds has posed a considerable challenge to valence theory [1]. Although a completely predictive understanding of the structures and electronic properties of cluster compounds has not been achieved, some useful and widely applicable generalisations have emerged, which rationalise the structures adopted by cluster compounds [2]. In particular, characteristic electron counts for certain topologically distinct classes of polyhedra, e.g. deltahedra, three-connected polyhedra, etc., have been recognised and are summarised in Table 1 for both Main Group and transition metal cluster compounds [3]. In addition, rules have been developed for larger cluster molecules derived by the condensation of the polyhedra listed in the Table through vertices, edges and faces [4].

Recently it has become apparent that some clusters adopt structures derived neither from deltahedra nor three-connected polyhedra but have structures based on four-connected polyhedra. Since this class of polyhedron has not been previously investigated from a theoretical point of view it was decided to make a systematic investigation of its electronic requirements.

Figure 1 illustrates some examples of four-connected polyhedra with 6 to 12 vertices. The first example, the octahedron, is of course also a deltahedron. Many of the other examples are edge duals of three-connected polyhedra [5]. The polyhedra

(a)–(d) are four-connected and additionally have the vertex atoms lying on a sphere. In contrast (e)–(g) are derived by capping three-connected polyhedra and for (f) and (g) this requires the simultaneous extension of some of the bonds in the parent polyhedron. For example, (f) is an elongated tricapped trigonal prism and (g) a tricapped cube with two edges lengthened. If all the bonds for (e)–(g) are constrained to be equal then the atoms lie on oblate or prolate spheroids. For these polyhedra a spherical distribution of atoms is only attained if the bond lengths are unequal.

The molecular orbital calculations which we have completed on (a)–(g) (see Appendix I for details) have suggested the following generalisations:

- (1) Spherical four-connected polyhedral molecules are characterised by a total of  $14n + 2$  valence electrons if the  $n$  vertex atoms are transition metals and  $4n + 2$  electrons if the vertex atoms are Main Group atoms.
- (2) Non-spherical four-connected polyhedral molecules are associated with variable electron counts of  $14n$  to  $14n + 4$  ( $4n$  to  $4n + 4$  for Main Group).

The first generalisation is most important because it demonstrates a coincidence in electron counts for deltahedral and four-connected polyhedral molecules. This coincidence can be readily interpreted in terms of Stone's Tensor Surface Harmonic Methodology [6]. Both classes of polyhedra have vertex atoms lying on the surface of a sphere and utilise common  $S^\sigma$ ,  $3P^\sigma/P^\pi$  and  $(n - 3)L^\pi$  radial and tangential molecular orbitals [7] (see Appendix I for details).

Three-connected transition metal polyhedral molecules are characterised by  $15n$  valence electrons ( $5n$  for Main Group) corresponding to the presence of  $3n/2$  skeletal MOs. In the Stone notation [6] these polyhedra have  $S^\sigma$ ,  $3P^\sigma/P^\pi$  and  $(n - 2)L^\pi$  strongly bonding MOs and  $(n - 2)L^\pi$  and  $\bar{L}^\pi$  parity matched non-bonding MOs [8]. The eclipsed arrangement of atoms in three-connected polyhedra leads to the occurrence of the non-bonding set, because interactions of the type illustrated in **1** have a cancelling effect. Bonding interactions between atoms on the same side

TABLE 1  
SUMMARY OF POLYHEDRAL SKELETAL ELECTRON PAIR APPROACH <sup>a</sup>

| Polyhedral type           | Polyhedral electron count (p.e.c.) |                |                  |                       |
|---------------------------|------------------------------------|----------------|------------------|-----------------------|
|                           | Main Group                         | Example        | Transition metal | Example <sup>b</sup>  |
| Deltahedra <i>closo-</i>  | $4n + 2$                           | $B_n H_n^{2-}$ | $14n + 2$        | $Os_5(CO)_{16}$       |
| <i>nido-</i>              | $4n + 4$                           | $B_n H_{n+4}$  | $14n + 4$        | $Ru_5C(CO)_{15}$      |
| <i>arachno-</i>           | $4n + 6$                           | $B_n H_{n+6}$  | $14n + 6$        | $[Os_4H_3I(CO)_{12}]$ |
| Three-connected polyhedra | $5n$                               | $C_n H_n$      | $15n$            | $Ir_4(CO)_{12}$       |
| Ring compounds            | $6n$                               | $C_n H_{2n}$   | $16n$            | $Os_3(CO)_{12}$       |

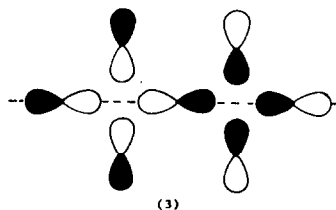
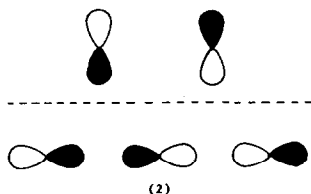
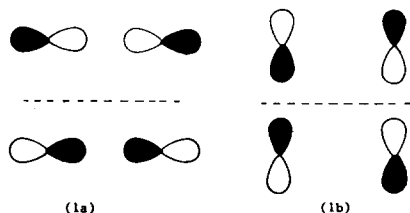
Condensed polyhedra derived from **A** (p.e.c. *a*) and **B** (p.e.c. *b*) <sup>c</sup>  
 Vertex shared  $a + b - 18$   
 Edge shared  $a + b - 34$   
 $\Delta$ -face shared  $a + b - 48$

<sup>a</sup> D.G. Evans and D.M.P. Mingos, *Organometallics*, 2 (1983) 435. <sup>b</sup> B.F.G. Johnson and J. Lewis, *Phil. Trans. R. Soc. Lond.*, A308 (1982) 5. <sup>c</sup> D.M.P. Mingos, *J. Chem. Soc., Chem. Commun.*, (1983) 706.

of the equator being balanced by antibonding interactions across the equator and vice versa. In four-connected polyhedral molecules these  $L^n$  orbitals are more strongly bonding and the  $\bar{L}^n$  orbitals more strongly antibonding. A situation which leads to a total of  $n + 1$  skeletal bonding MOs. The  $L^n$ 's are stabilised by interactions of the type shown in **2** and **3**. Those in **2** occur in situations where the atoms adopt a staggered arrangement, and those in **3** where there are additional atoms on the equator. The *parity transformation* [6] leads to a corresponding set of  $\bar{L}^n$  antibonding orbitals.

Interestingly the rhombic dodecahedron (**4**) which has 10 four-connected and 4 three-connected vertices also conforms to the  $14n + 2$  rule, because the vertex atoms adopt a staggered arrangement about the equator.  $[\text{Rh}_{15}(\text{CO})_{30}]^{3-}$  has a rhombic dodecahedral geometry [9] and the expected electron count of 198. It can also be viewed as an elongated tetracapped cube.

For the borane anions,  $\text{B}_n\text{H}_n^{2-}$ , the deltahedral geometries are generally more stable than the alternative four-connected geometries, because they maximise the number of nearest neighbour resonance integral terms [6]. For transition metal cluster compounds, where the potential energy surfaces connecting alternative polyhedral geometries are softer and ligand interaction terms can compete with the metal-metal bonding terms, then four-connected polyhedral structures are also



observed. Examples of deltahedral and four-connected polyhedral transition metal cluster compounds are contrasted in Table 2. Both types of polyhedral molecule occur with equal frequency. For the twelve vertex situation examples of both polyhedral types have been characterised, viz.  $[\text{Rh}_{12}\text{Sb}(\text{CO})_{27}]^{3-}$  – icosahedral [10] and  $[\text{Rh}_{13}\text{H}_{5-n}(\text{CO})_{24}]^{n-}$  – twinned cuboctahedral [11].

The square-antiprism (b) represents a particularly interesting example since as a four-connected polyhedron it is expected to conform to the  $14n + 2$  rule, i.e. have 114 valence electrons. It is additionally an *arachno*-bicapped square-antiprism, which is associated with  $14n + 6$  valence electrons (118) [3]. Examples of clusters with both electron counts have been characterised, i.e.  $[\text{Co}_8\text{C}(\text{CO})_{18}]^{2-}$  and  $[\text{Ni}_8\text{C}(\text{CO})_{16}]^{2-}$  the former showing a slight distortion towards the alternative deltahedral structure [12]. The fluxionality of  $\text{B}_8\text{H}_8^{2-}$  can also be related to the

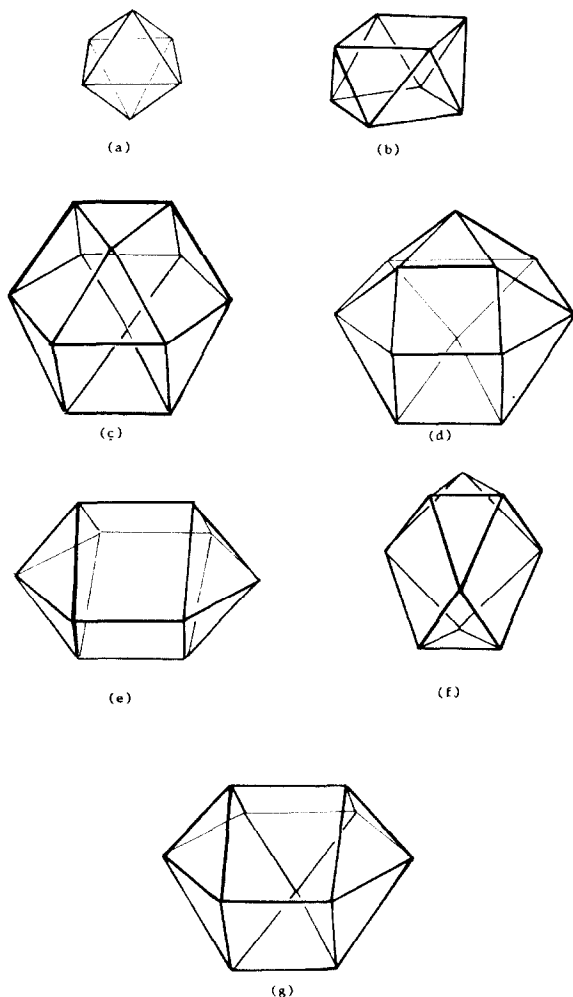
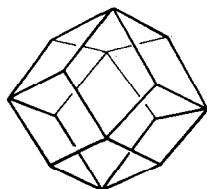


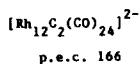
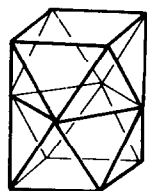
Fig. 1. Some examples of four-connected polyhedra. (a) octahedron, (b) square-antiprism, (c) cuboctahedron, (d) twinned cuboctahedron, (e) bicapped cube, (f) elongated tricapped trigonal prism, and (g) four-connected tridecahedron.

occurrence of alternative square-antiprismatic and bicapped trigonal prismatic structures with similar valence electron requirements and energies [13].

The  $14n + 2$  rule for four-connected polyhedral molecules can be combined with the previously developed condensation rules [4] to build up higher nuclearity cluster molecules. For a pair of polyhedra (**A** and **B**) sharing a common square face the polyhedral electron count (p.e.c.) is  $a + b - 62$ , where  $a$  and  $b$  are the p.e.c.'s characteristic of **A** and **B** and 62 is the electron count associated with the common square face. Examples of condensed polyhedral molecules of this type are illustrated in (5)–(7). The basis of the condensation rule for four-connected polyhedra is discussed in more detail in Appendix II. In deriving the p.e.c.'s for 5–7 the capped trigonal prismatic and trigonal bipyramidal fragments were assigned p.e.c.'s of 102 and 72 respectively [3,4]. The skeletal geometries illustrated for 5–7 are somewhat idealised representation of the observed structures established for  $[\text{Rh}_{12}\text{C}_2(\text{CO})_{24}]^{2-}$ ,

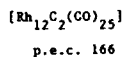
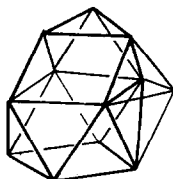


(4)



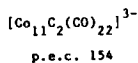
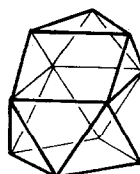
face sharing pair  
of sq. antiprisms

(5)



capped fused trigonal  
prism-sq. antiprism and  
trigonal bipyramid

(6)



trigonal prism  
and square antiprism

(7)

$[\text{Rh}_{12}\text{C}_2(\text{CO})_{25}]$  and  $[\text{Co}_{11}\text{C}_2(\text{CO})_{22}]^{3-}$  and follow from the descriptions of Teo et al. [14]. There are alternative descriptions of these structures not based on four-connected polyhedra. For example, 5 can be described as a pair of bicapped trigonal prisms (p.e.c. 114) sharing a common flat butterfly face (p.e.c. 62) and thereby introducing an additional bond across the central rhombus of metal atoms. Such a cluster is also consistent with the condensation rules and more accurately represents the structure. Similarly, 6 and 7 can be described in terms of a central cube, with a broken bond, capped by either three or four metal atoms. Clearly for these higher

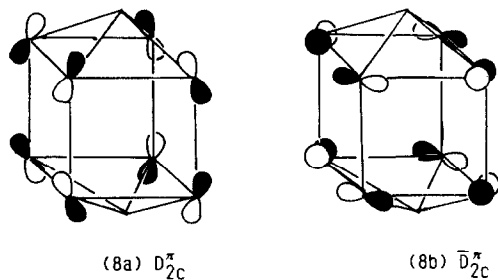
TABLE 2  
 EXAMPLES OF DELTAHEDRAL AND FOUR-CONNECTED TRANSITION METAL CLUSTERS

| <i>n</i> | 14 <i>n</i> + 2 | Deltahedral               |  | Four-connected                         |   | Ref.           |
|----------|-----------------|---------------------------|--|--|---|----------------|
|          |                 | Geometry                  | Example  | Geometry                               | Example   |                |
| 6        | 86              | Octahedral                | Rh <sub>6</sub> (CO) <sub>16</sub>                     | Octahedral                             | Rh <sub>6</sub> (CO) <sub>16</sub>                                    | <sup>a</sup>   |
| 7        | 100             | Pentagonal-bipyramid      |  |  |   |                |
| 8        | 114             | Dodecahedron              |  | Square anti-prism                      | [Co <sub>8</sub> C(CO) <sub>18</sub> ] <sup>2-</sup>                  | <sup>b</sup>   |
| 9        | 128             | Tricapped trigonal prism  |  |  |   |                |
| 10       | 142             | Bicapped square antiprism | [Rh <sub>10</sub> P(CO) <sub>22</sub> ] <sup>3-</sup>  |  |   | <sup>c</sup>   |
| 12       | 170             | Icosahedron               | [Rh <sub>12</sub> Sb(CO) <sub>27</sub> ] <sup>3-</sup> | Twinned cuboctahedron<br>Cuboctahedron | [Rh <sub>13</sub> (CO) <sub>24</sub> H <sub>5-n</sub> ] <sup>n-</sup> | <sup>d,e</sup> |

<sup>a</sup> E.R. Corey, L.F. Dahl and W. Beck, *J. Amer. Chem. Soc.*, 85 (1963) 1202. <sup>b</sup> V.G. Albano, P. Chini, G. Ciani, S. Martinengo and M. Sansoni, *J. Chem. Soc., Dalton Trans.*, (1978) 468. <sup>c</sup> J.L. Vidal, W.E. Walker and R.C. Schoening, *Inorg. Chem.*, 20 (1981) 238. <sup>d</sup> J.L. Vidal and J.M. Troup, *J. Organomet. Chem.*, 213 (1981) 351. <sup>e</sup> G. Ciani, A. Sironi and S. Martinengo, *J. Chem. Soc., Dalton Trans.*, (1981) 519.

nuclearity clusters there are many alternative structures consistent with the condensation rules. A systematic method of analysing these possibilities has recently been developed [15].

The non-spherical four-connected polyhedral molecules (f)–(g) are related by capping processes to three-connected polyhedra. In a previous paper [8] we established that the latter have a set of (*n* – 2) non-bonding *L*<sup>π</sup> and  $\bar{L}^{\pi}$  molecular orbitals. The addition of capping atoms can stabilise some of these molecular orbitals, but for (e) a pair of matching *D*<sub>2c</sub><sup>π</sup> and  $\bar{D}$ <sub>2c</sub><sup>π</sup> molecular orbitals are unaffected by the capping process and remain essentially non-bonding. These parity matched molecular orbitals are illustrated in 8. It is the occurrence of this almost non-bonding pair of molecular orbitals which permits this molecule to have electron counts in the range 14*n* to 14*n* + 4 (4*n* to 4*n* + 4 for Main Group elements). Related pairs of non-bonding *L*<sup>π</sup> and  $\bar{L}^{\pi}$  MO's are observed for the other non-spherical four-connected polyhedra, although in some instances, e.g. (f), the MOs are localised more on the capping



atoms than the parent polyhedron. To date no examples of such cluster compounds have been structurally characterised, but clearly (f) is closely related to the tricapped trigonal prism for which molecules with 4*n* + 2 and 4*n* + 4 electrons have been characterised [8].

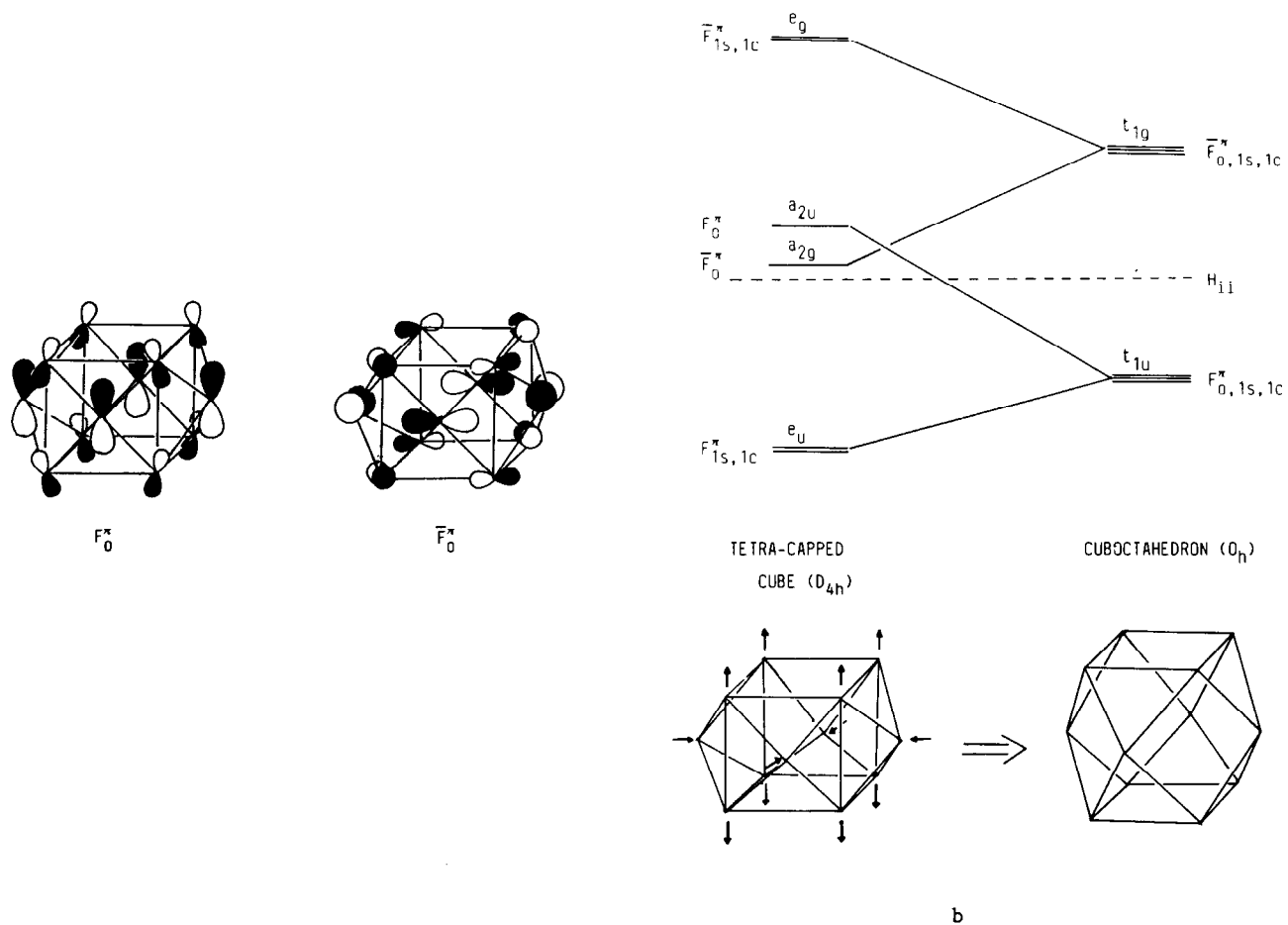


Fig. 2. (a) Illustration of the  $F_0^*$  and  $\bar{F}_0^*$  orbitals. (b) A correlation diagram for the frontier orbitals for the interconversion of a tetra-capped cube and a cuboctahedron are illustrated. As the polyhedron becomes more spherical the energies of the  $F_0^*$  and  $\bar{F}_0^*$  molecular orbitals diverge.

The tetracapped cube ( $D_{4h}$  symmetry) has a pair of approximately non-bonding  $F_0^\pi$  and  $\bar{F}_0^\pi$  molecular orbitals, which are illustrated in Fig. 2(a). The occurrence of these orbitals permits electron counts in the range  $14n$  to  $14n + 4$  (or  $4n$  to  $4n + 4$  for Main Group clusters) [8]. The tetracapped cube defines an oblate spheroid, but can be converted into a spherical polyhedron, the cuboctahedron, by simultaneously stretching along the four-fold axis and compressing in the equatorial directions. The correlation diagram in Fig. 2(b) demonstrates that this distortion results in a stabilisation of  $F_0^\pi$  and a destabilisation of  $\bar{F}_0^\pi$  and a preferred electron count of  $14n + 2$  for the cuboctahedron. This correlation diagram emphasises the important bonding distinction between those clusters which have spherical and non-spherical dispositions of vertex atoms.

### Acknowledgements

The S.E.R.C. is thanked for financial support.

### Appendix I

Extended Hückel molecular orbital calculations were performed on the four-connected polyhedral molecules illustrated in Fig. 1 [6]. Since the  $14n + 2 - 4n + 2$  relationship which connects transition metal carbonyl and Main Group clusters arises because of the correspondence in antibonding molecular orbitals it is more economical in terms of computer time to perform the calculations on model  $B_n H_n^{2-}$  compounds. The B-B bond lengths were set equal to 1.70 and B-H to 1.00 Å.

#### PARAMETERS USED IN CALCULATIONS

| Atom | Orbital | $H_{ii}$ (eV) | $\zeta$ |
|------|---------|---------------|---------|
| B    | 2s      | -15.20        | 1.30    |
|      | 2p      | -8.50         | 1.30    |
| H    | 1s      | -13.60        | 1.30    |

The Extended Hückel constant was set equal to 1.75.

#### SUMMARY OF BONDING AND NON-BONDING MOLECULAR ORBITALS FOR THE POLYHEDRAL $B_n H_n^{2-}$ MOLECULES ILLUSTRATED IN FIG. 1 AND RELATED CAPPED THREE-CONNECTED POLYHEDRA

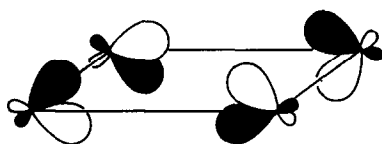
| $n$ | Geometry                       | Radial and tangential skeletal molecular orbitals   |  |
|-----|--------------------------------|---|--|
|     |                                | Bonding   | Non-bonding  |
| 6   | Octahedral                     | $S^\sigma(a_{1g})P^\sigma(t_{1u})D_{1s,1c,2s}^\pi(t_{2g})$  |  |
| 8   | Square-antiprism               | $S^\sigma(a_1)P^\sigma(a_2e_1)D_0^\sigma(a_1)D_{1s,1c}^\pi(e_2)$  | $D_{2s,2c}^\pi(e_3)$<br>$\bar{D}_{2s,2c}^\pi(e_1)$ |
| 9   | Tricapped trigonal prism (ttp) | $S^\sigma(a'_1)P^\sigma(a'_2e')D^\pi(a'_1e'e'')$  | $F_0^\pi(a'_2)\bar{F}_0^\pi(a'_2)$                 |
| 9   | Elongated ttp                  | Same as ttp but $F_0^\pi(a'_2)$ bonding $\bar{F}_0^\pi(a'_2)$ antibonding   |  |
| 10  | Bicapped cube                  | $S^\sigma(a_{1g})P^\sigma(a_{2u}e_u)D_0^\sigma(a_{1g})D_{1s,1c}^\pi(e_g)$<br>$D_{2s}^\pi(b_{2g})F_{1s,1c}^\pi(e_u)$ | $D_{2c}^\pi(b_{1g})\bar{D}_{2c}^\pi(b_{1u})$       |
| 12  | Cuboctahedron                  | $S^\sigma(a_{1g})P^\sigma(t_{1u})D^\pi(e_g t_{2g})$<br>$F_{0,1s,1c}^\pi(t_{1u})F_{2c}^\pi(a_{2u})$                  |  |
| 12  | Twinned cuboctahedron          | $S^\sigma(a'_1)P^\sigma(a'_2e')D^\pi(a'_1e'e'')$<br>$F_{0,1s,1c}^\pi(a'_2e')F_{3c}^\pi(a'_1)$                       |  |
| 12  | Tetracapped cube               | $S^\sigma(a_{1g})P^\sigma(a_{2u}e_u)D^\pi(a_{1g}e_g b_{2g} b_{1g})$<br>$F_{1s,1c}^\pi(e_u)F_{2c}^\pi(b_{1u})$       | $F_0^\pi(a_{2u})\bar{F}_0^\pi(a_{2g})$             |



## Appendix II

The correspondence between electron counting rules for deltahedral boranes and transition metal carbonyl clusters with  $n$  vertices can be related to the occurrence in both classes of molecules of  $2n - 1$  inaccessible antibonding molecular orbitals localised predominantly on the metal [6,17]. Their inaccessibility arises either from their high energies, or from their hybridisation towards the centre of the cluster which makes them unsuitable for metal–ligand bond formation. The electron counting rules can in addition be extended to condensed clusters derived by vertex, edge or triangular face sharing of deltahedral clusters [4]. For four-connected polyhedral clusters the possibility of condensation through square faces also arises.

A four-connected polyhedral cluster with  $n$  atoms also has  $2n - 1$  inaccessible antibonding orbitals [6]. The removal of  $x$  atoms from the cluster leads to two fragments each with their characteristic sets of inaccessible antibonding orbitals [6]. The loss of a single atom ( $x = 1$ ) leads to a *nido*-fragment and an atom which can accommodate 9 electron pairs around it, i.e. it has no inaccessible antibonding metal–metal MOs and  $X = 0$ . The loss of an edge generates an *arachno*-fragment and a dimer with a single antibonding metal–metal MO, i.e.  $X = 1$ . The loss of a triangle generates a *hypho*-fragment and a triangular cluster, which if saturated has 3 antibonding metal–metal  $\sigma^*$  MOs, i.e.  $X = 3$ . For the loss of a square face this reasoning suggests that  $X$  will equal 4 corresponding to the presence of four antibonding metal–metal MOs. However, such a fragment also has an out of plane  $\pi^*$  orbital (9) which is sufficiently high lying to also be inaccessible, i.e. for  $x = 4$ ,  $X = 4$  or 5. The remaining *nido*-, *arachno*-, etc. fragments are now characterised by



(9)

$(2n - 1) - X$  MOs. If a condensed cluster is formed by bringing together two depleted fragments with  $(n - x)$  and  $(m - x)$  atoms the total number of inaccessible orbitals is  $(2n - 1 - X)$  plus  $(2m - 1 - X)$  and  $X$  for the common fragment, making  $(2n - 1) + (2m - 1) - X$ .

This leads to the condensation rule:

*The total electron count in a condensed cluster is equal to the sum of the characteristic electron counts for the parent polyhedra minus the electron count characteristic of the atom pair of atoms or face of atoms common to both polyhedra*

The  $X$  values described above lead to the following characteristic electron counts for the common moieties: vertex 18, edge 34, and triangle 48. For a square the ambiguity in  $X$  value described above leads to an electron count of 64 if  $X = 4$  and 62 if  $X = 5$ . For the clusters described in this paper where the bonding is not

localised to the edges of the polyhedra the latter value of  $X$  is appropriate. However, when condensation of three-connected polyhedra through square faces occurs then the former is appropriate since the 64 electron count corresponds to a localised description of the bonding around the square face.  $[\text{Co}_6\text{Ni}_2\text{C}_2(\text{CO})_{16}]^{2-}$ , which has a structure based on two trigonal prisms sharing a common square face provides an example of such a localised bonding description [18].

## References

- 1 Transition Metal Clusters, B.F.G. Johnson (Ed.), Wiley, New York, 1980 gives a good introduction to transition metal cluster Chemistry.
- 2 K. Wade, *Adv. Inorg. Chem. Radiochem.*, 18 (1976) 1; D.M.P. Mingos, *Nature Phys. Sci. (London)*, 236 (1972) 99.
- 3 D.G. Evans and D.M.P. Mingos, *Organometallics*, 2 (1983) 435.
- 4 D.M.P. Mingos, *J. Chem. Soc., Chem. Commun.*, (1983) 706; D.M.P. Mingos, *Acc. Chem. Res.*, 17 (1984) 311.
- 5 Algebraic Graph Theory, N. Biggs, Cambridge University Press, London, 1974.
- 6 A.J. Stone, *Mol. Phys.*, 41 (1980) 1339; A.J. Stone, *Inorg. Chem.*, 20 (1981) 563; A.J. Stone and M.J. Alderton, *Inorg. Chem.*, 21 (1982) 2297; A.J. Stone, *Polyhedron*, 280 (1985) 407.
- 7 P. Brint, J.P. Cronin and E. Seward, *J. Chem. Soc., Dalton Trans.*, (1983) 675.
- 8 R.L. Johnston and D.M.P. Mingos, *J. Organomet. Chem.*, 280 (1985) 407.
- 9 J.L. Vidal, L.A. Kapicak and J.M. Troup, *J. Organomet. Chem.*, 215 (1981) C11.
- 10 J.L. Vidal and J.M. Troup, *J. Organomet. Chem.*, 213 (1981) 351.
- 11 G. Ciani, A. Sironi and S. Martinengo, *J. Chem. Soc., Dalton Trans.*, (1981) 519.
- 12 V.G. Albano, P. Chini, G. Ciani, S. Martinengo and M. Sansoni, *J. Chem. Soc., Dalton Trans.*, (1978) 463.
- 13 E.L. Muetterties, R.J. Wiersema and M.F. Hawthorne, *J. Amer. Chem. Soc.*, 95 (1973) 7520; D.R. Eaton, L.J. Guggenberger and E.L. Muetterties, *Inorg. Chem.*, 6 (1967) 1271.
- 14 B.K. Teo, G. Longoni and F.R.K. Chung, *Inorg. Chem.*, 23 (1984) 1257.
- 15 M. McPartlin and D.M.P. Mingos, *Polyhedron Symposia In Print*, in press.
- 16 R. Hoffmann and W.N. Lipscomb, *J. Chem. Phys.*, 36 (1962) 2179; R. Hoffmann, *J. Chem. Phys.*, 39 (1963) 1397; J. Howell, A. Rossi, D. Wallace, K. Haraki and R. Hoffmann, *QCPE*, 10 (1977) 344.
- 17 D.M.P. Mingos, *J. Chem. Soc., Dalton Trans.*, (1974) 133.
- 18 G. Longoni, A. Ceriotti, R. Della Pergola, M. Manasserro and M. Sansoni, unpublished results quoted in ref. 14.